

Recurrent Equilibrium Networks: Flexible Dynamic Models with Guaranteed Stability and Robustness

Max Revay, Ruigang Wang, Ian R. Manchester

Abstract—This paper introduces *recurrent equilibrium networks* (RENs), a new class of nonlinear dynamical models for applications in machine learning, system identification and control. The new model class has “built in” guarantees of stability and robustness: all models in the class are contracting – a strong form of nonlinear stability – and models can satisfy prescribed incremental integral quadratic constraints (IQC), including Lipschitz bounds and incremental passivity. RENs are otherwise very flexible: they can represent all stable linear systems, all previously-known sets of contracting recurrent neural networks and echo state networks, all deep feedforward neural networks, and all stable Wiener/Hammerstein models. RENs are parameterized directly by a vector in \mathbb{R}^N , i.e. stability and robustness are ensured without parameter constraints, which simplifies learning since generic methods for unconstrained optimization can be used. The performance and robustness of the new model set is evaluated on benchmark nonlinear system identification problems, and the paper also presents applications in data-driven nonlinear observer design and control with stability guarantees.

I. INTRODUCTION

Deep neural networks (DNNs), recurrent neural networks (RNNs), and related models have revolutionised many fields of engineering and computer science [1]. Their apparent flexibility, accuracy, and scalability have led to renewed interest in neural networks, and more generally learning and data-driven methods, in control, identification, and related areas [2]–[4].

On the other hand, it has been observed that neural networks can be very sensitive to small changes in inputs [5], and this sensitivity can extend to control policies [6]. Furthermore, their scale and complexity makes them difficult to certify for use in many control systems applications, which is especially problematic for safety-critical systems, and it can be difficult to incorporate prior physical knowledge into a neural network model, e.g. that a model should be stable.

The most accurate current methods for certifying stability and robustness of DNNs and RNNs are based on mixed-integer programming [7] and semidefinite programming [8], [9] which face challenges when scaling to large networks. Additionally, these methods have been developed for analysing a fixed neural network after training, but enforcing these constraints during training has required solving constrained optimization problems [10], [11].

This work was supported by the Australian Research Council.

The authors are with the Australian Centre for Field Robotics and Sydney Institute for Robotics and Intelligent Systems, The University of Sydney, Sydney, NSW 2006, Australia (e-mail: ian.manchester@sydney.edu.au).

In this paper, we introduce a new model structure: the *recurrent equilibrium network* (REN).

- 1) RENs are highly *flexible* and include many standard models as special cases, including DNNs, RNNs, echo-state networks and stable linear dynamical systems.
- 2) RENs have *built in guarantees* of stability, robustness or other properties that are relevant to safety critical systems or physics informed learning.
- 3) RENs are *easy to use* as they permit a direct (unconstrained) parametrisation enabling learning of large-scale models via simple first-order methods such as stochastic gradient descent.

RENs are guaranteed to be contracting [12], a strong form of nonlinear stability, and their built-in robustness guarantees take the form of incremental integral quadratic constraints (IQCs) [13]. This class of constraints includes user-definable bounds on the Lipschitz constant (incremental gain) of the network, and the IQC framework is inherently compatible with many commonly used tools for certifying system interconnection, including passivity methods in robotics [14], networked-system analysis via dissipation inequalities [15], μ analysis [16], and standard tools for analysis of nonlinear control systems [17]. The code to run all experiments is available via the following link github.com/imanchester/REN.

A. Learning and Identification of Stable Models

The problem of learning dynamical systems with stability guarantees appears frequently in system identification. When learning models with feedback it is not uncommon for the model to be unstable even if the data-generating system is stable. Even in the case of linear models, guaranteeing stability of identified models is complicated by the fact that the set of stable matrices is non-convex, and various methods have been proposed to guarantee stability via regularization and constrained optimization [18]–[24].

For nonlinear models, there has also been a substantial volume of research on stability guarantees, e.g. for polynomial models [25]–[28], Gaussian mixture models [29], and recurrent neural networks [10], [23], [30]–[32]. However, the problem is substantially more complex than the linear case due to the many different definitions of nonlinear stability. Indeed, even verification of stability of a given model is challenging. Contraction is a strong form of nonlinear stability [12] which is particularly well-suited to problems in learning and system identification since it guarantees stability of *all* solutions of

the model, irrespective of inputs or initial conditions. This is important in learning since the purpose of a model is to simulate responses to previously unseen inputs. In particular, the works [10], [25]–[28], [30], [32] are guaranteed to find contracting models.

B. Robustness Certification of Neural Networks

Beyond stability, model *robustness* can be characterized in terms of sensitivity to small perturbations in the input. It has recently been shown that recurrent neural network models can be extremely fragile [33], i.e. small changes to the input produce dramatic changes in the output.

Formally, sensitivity and robustness can be quantified via *Lipschitz bounds* on the input-output mapping defined by the model, e.g. incremental ℓ_2 gain bounds and related properties such as incremental passivity, which have a long history in systems analysis [34]. In machine learning, Lipschitz constants are used in the proofs of generalization bounds [35], analysis of expressiveness [36] and guarantees of robustness to adversarial attacks [37], [38]. There is also ample empirical evidence to suggest that Lipschitz regularity (and model stability, where applicable) improves generalization in machine learning [39], system identification [32] and reinforcement learning [40].

Unfortunately, even calculation of the Lipschitz constant of a feedforward (static) neural networks is NP-hard [41] and instead approximate bounds must be used. The tightest bound known to date is found by using quadratic constraints to construct a behavioural description of the neural network activation functions [42]. Extending this approach to network synthesis (i.e., training new neural networks with a prescribed Lipschitz bound) is complicated by the fact that model parameters and IQC multipliers are not jointly convex. In [11], Lipschitz bounded feedforward models were trained using the Alternating Direction Method of Multipliers, and in [32], a convexifying implicit parametrization and an interior point method were used to train Lipschitz bounded recurrent neural networks. Empirically, both works suggest generalisation and robustness advantages to Lipschitz regularisation, however, the requirements to satisfy linear matrix inequalities at each iteration mean that these methods are limited to relatively small scale networks.

C. Applications of Stable and Robust Models in Data-Driven Control and Estimation

Beyond system identification, the ability to learn flexible dynamical models with contraction, robustness and behavioural constraints has many applications in control and related fields, some of which we explore in this paper.

The problem of nonlinear observer design (state estimation) can be posed as the search for a contracting dynamical system that can reproduce true system trajectories [43] [44]. In this paper, we formulate the observer design problem as a supervised learning problem over a set of contracting nonlinear systems, and apply it to a nonlinear reaction diffusion PDE.

In optimization of linear controllers, a classical and widely-used approach is via the Youla-Kucera (or Q) parameterization, which represents all stabilizing controllers for a given system

via a “free” stable system [16], [45]. This approach can be extended to nonlinear systems [46], [17] in which the “free parameter” is a stable nonlinear model. In this paper, we show how learning over stable nonlinear models can be used to optimize nonlinear feedback policies for constrained linear control. This can be considered a data-driven approach to explicit model predictive control [47] with stability guarantees.

Beyond these settings, there are many further applications of flexible models with stability and robustness guarantees. In reinforcement learning [48], it has recently been found that the Lipschitz constant of policies has a strong effect on their robustness to adversarial attack [40]. In robotics, many approaches to control use passivity constraints to ensure stable interactions with physical environments, e.g. [49], [50]. In [51] it was shown that privacy preservation in dynamic feedback policies can be represented as an incremental ℓ^2 gain bound, and thus the models we present here can be used for learning feedback policies with privacy guarantees.

D. Convex and Direct Parameterizations

In this paper we provide convex parameterizations of contracting and robust RENs via linear matrix inequality (LMI) constraints, building upon our recent paper [10]. Although convex, LMIs can be computationally challenging to incorporate for large-scale models. For example, a path-following interior point method, as proposed in [10] generally requires computing gradients of barrier functions, line search procedures, and a combination of “inner” and “outer” iterations as the barrier parameter changes.

A major benefit of RENs is that we can also provide *direct* i.e. unconstrained parameterizations of contracting and robust models. That is, we construct a smooth mapping from \mathbb{R}^N to the model weights such that every model in the image of this mapping satisfies the desired behavioural constraints.

The approach is somewhat similar to the method of [52] for semidefinite programming, in which a positive-semidefinite matrix X is represented by its factors $X = VV^T$, so that V can be treated as a “free” variable ensuring $X \succeq 0$. Despite introducing non-convexity, this approach has proven to be beneficial for large-scale semidefinite programming problems. Our parameterization differs in that the method of [52] generally requires nonlinear equality constraints to be satisfied, whereas in our method the associated optimization problems are completely unconstrained. The major benefit of this is that a wide variety of algorithms from unconstrained optimization can be directly applied, e.g. methods such as stochastic gradient descent and Adam [53] that have been developed for large-scale machine learning applications.

Another advantage of a direct parameterization is that it allows easy *random sampling* of nonlinear models with the required stability and robustness constraints. In this sense, our parameterization is also similar in spirit to that proposed in [54] for randomized design of robust linear control systems, and also has application to the generation of *echo state networks*, i.e. large-scale recurrent networks with fixed dynamics and learnable output maps (see, e.g., [55], [56] and references therein).

E. Structure of this Paper

The paper structure is as follows:

- Sections II - VI discuss the proposed model class and its properties. Section II formulates the problem of learning stable and robust dynamical models; in Section III we present the REN model class; in Section IV we present convex parameterizations of stable and robust RENs; in Section V we present direct (unconstrained) parameterisations of RENs; in Section VI we discuss the expressivity of the REN model class, showing it includes many commonly-used models as special cases.
- Sections VII - IX present applications of learning stable/robust nonlinear models. Section VII presents applications to system identification; Section VIII presents applications to nonlinear observer design; Section IX presents applications to nonlinear feedback design for linear systems.

Preliminary work related to this paper was presented in the conference submission [57]. The present work expands on this by expanding the class of robustness properties, removing restrictions on the model weights, and presenting applications in observer design and control, as well as further comparisons in system identification.

F. Notation

The set of sequences $x : \mathbb{N} \rightarrow \mathbb{R}^n$ is denoted by ℓ_{2e}^n . Superscript n is omitted when it is clear from the context. For $x \in \ell_{2e}^n$, $x_t \in \mathbb{R}^n$ is the value of the sequence x at time $t \in \mathbb{N}$. The subset $\ell_2 \subset \ell_{2e}$ consists of all square-summable sequences, i.e., $x \in \ell_2$ if and only if the ℓ_2 norm $\|x\| := \sqrt{\sum_{t=0}^{\infty} |x_t|^2}$ is finite, where $|\cdot|$ denotes Euclidean norm. Given a sequence $x \in \ell_{2e}$, the ℓ_2 norm of its truncation over $[0, T]$ is $\|x\|_T := \sqrt{\sum_{t=0}^T |x_t|^2}$. We use $A \succ 0$ and $A \succeq 0$ to denote a positive definite and positive semi-definite matrix, respectively. We denote the set of positive-definite diagonal matrices by \mathbb{D}_+ .

II. LEARNING STABLE AND ROBUST MODELS

This paper is concerned with *learning* of nonlinear dynamical models, i.e. finding a particular model within a set of candidates based on some *data*. The overall objective is to construct models that are *flexible* enough to make use of available data, and yet *guaranteed* to be well-behaved in some sense.

Given a dataset \tilde{z} , we consider the problem of learning a nonlinear state-space dynamical model of the form

$$x_{t+1} = f(x_t, u_t, \theta), \quad y_t = g(x_t, u_t, \theta) \quad (1)$$

that minimizes some loss or cost function depending (in part) on the data, i.e. to solve a problem of the form

$$\min_{\theta \in \Theta} \mathcal{L}(\tilde{z}, \theta). \quad (2)$$

In the above, $x_t \in \mathbb{R}^n$, $u_t \in \mathbb{R}^m$, $y_t \in \mathbb{R}^p$, $\theta \in \Theta \subseteq \mathbb{R}^N$ are the model state, input, output and parameters, respectively. Here $f : \mathbb{R}^n \times \mathbb{R}^m \times \Theta \rightarrow \mathbb{R}^n$ and $g : \mathbb{R}^n \times \mathbb{R}^m \times \Theta \rightarrow \mathbb{R}^p$ are piecewise continuously differentiable functions.

Example 1: In the context of system identification we may have $\tilde{z} = (\tilde{y}, \tilde{u})$ consisting of finite sequences of input-output measurements, and aim to minimize *simulation error*:

$$\mathcal{L}(\tilde{z}, \theta) = \|y - \tilde{y}\|_T^2 \quad (3)$$

where $y = \mathfrak{R}_a(\tilde{u})$ is the output sequence generated by the nonlinear dynamical model (1) with initial condition $x_0 = a$ and inputs $u_t = \tilde{u}_t$. Here the initial condition a may be part of the data \tilde{z} , or considered a learnable parameter in θ .

In this paper, we are primarily concerned with constructing model parameterizations that have favourable stability and robustness properties, and we make the following definitions:

Definition 1: A model parameterization (1) is called a *convex parameterization* if $\Theta \subseteq \mathbb{R}^N$ is a convex set. Furthermore, it is called a *direct parameterization* if $\Theta = \mathbb{R}^N$.

Direct parameterizations are useful for learning large-scale models since many scalable unconstrained optimization methods (e.g. stochastic gradient descent) can be applied to solve the learning problem (2).

The particular form of nonlinear stability we use is the following:

Definition 2: A model (1) is said to be *contracting* if for any two initial conditions $a, b \in \mathbb{R}^n$, given the same input sequence $u \in \ell_{2e}^m$, the state sequences x^a and x^b satisfy

$$|x_t^a - x_t^b| \leq K\alpha^t |a - b|$$

for some $K > 0$ and $\alpha \in [0, 1)$.

Roughly speaking, contracting models forget their initial conditions exponentially, which is useful for system identification and state estimation. It is also desirable to learn a stable model with certain robustness properties.

Definition 3: A model (1) is said to satisfy the *incremental integral quadratic constraint* (IQC) defined by (Q, S, R) where $0 \succeq Q \in \mathbb{R}^{p \times p}$, $S \in \mathbb{R}^{m \times p}$, and $R = R^\top \in \mathbb{R}^{m \times m}$, if for all pairs of solutions with initial conditions $a, b \in \mathbb{R}^n$ and input sequences $u, v \in \ell_{2e}^m$, the output sequences $y^a = \mathfrak{R}_a(u)$ and $y^b = \mathfrak{R}_b(v)$ satisfy

$$\sum_{t=0}^T \begin{bmatrix} y_t^a - y_t^b \\ u_t - v_t \end{bmatrix}^\top \begin{bmatrix} Q & S^\top \\ S & R \end{bmatrix} \begin{bmatrix} y_t^a - y_t^b \\ u_t - v_t \end{bmatrix} \geq -d(a, b), \quad \forall T \quad (4)$$

for some function $d(a, b) \geq 0$ with $d(a, a) = 0$.

Important special cases of incremental IQCs include:

- $Q = -\frac{1}{\gamma}I, R = \gamma I, S = 0$: the model satisfies an ℓ^2 Lipschitz bound, a.k.a. incremental ℓ^2 -gain bound, of γ :

$$\|\mathfrak{R}_a(u) - \mathfrak{R}_a(v)\|_T \leq \gamma \|u - v\|_T, \quad \forall u, v \in \ell_{2e}^m, T \in \mathbb{N}.$$

- $Q = 0, R = -2\nu I, S = I$ where $\nu \geq 0$: the model is incrementally input passive:

$$\sum_{t=0}^T (\mathfrak{R}_a(u_t) - \mathfrak{R}_a(v_t))^\top (u_t - v_t) \geq \nu \|u - v\|_T^2$$

for all $u, v \in \ell_{2e}^m$ and $T \in \mathbb{N}$.

- $Q = -2\rho I, R = 0, S = I$ where $\rho > 0$: the model is incrementally strictly output passive:

$$\sum_{t=0}^T (\mathfrak{R}_a(u_t) - \mathfrak{R}_a(v_t))^\top (u_t - v_t) \geq \rho \|\mathfrak{R}_a(u) - \mathfrak{R}_a(v)\|_T^2$$

for all $u, v \in \ell_{2e}^m$ and $T \in \mathbb{N}$.

In other contexts, Q, S, R may be decision variables in a separate optimization problem to validate stability of inter-connected systems.

Remark 1: Given a model class guaranteeing incremental IQC defined by constant matrices Q, S, R , it is straightforward to construct models satisfying *frequency-weighted* IQCs. E.g. by constructing a model \mathfrak{R} that is contracting and satisfies an ℓ^2 Lipschitz bound, and choosing stable linear filters W_1, W_2 , with W_1 having a stable inverse, the new model

$$y = \mathfrak{W}_a(u) = W_1^{-1} \mathfrak{R}_a(W_2 u)$$

is contracting and satisfies the frequency-weighted bound

$$\|W_1(\mathfrak{W}_a(u) - \mathfrak{W}_a(v))\|_T \leq \gamma \|W_2(u - v)\|_T.$$

This can be useful e.g. if a model should be sensitive over only a selected range of frequencies.

III. RECURRENT EQUILIBRIUM NETWORKS

The model structure we propose – the *recurrent equilibrium network* (REN) – is a state-space model of the form (1) with

$$x_{t+1} = Ax_t + B_1 w_t + B_2 u_t + b_x, \quad (5)$$

$$y_t = C_2 x_t + D_{21} w_t + D_{22} u_t + b_y, \quad (6)$$

where w_t is the solution of an *equilibrium network*, a.k.a. *implicit network* [58]–[61]:

$$w_t = \sigma(D_{11} w_t + C_1 x_t + D_{12} u_t + b_w) \quad (7)$$

and σ is a scalar nonlinearity applied elementwise. We will show below how to ensure that a unique solution w_t^* to (7) exists and can be computed efficiently. The term “equilibrium” comes from the fact that any solution of the above implicit equation is also an equilibrium point of the difference equation $w_t^{k+1} = \sigma(D_{11} w_t^k + b_w)$ or the ordinary differential equation $\frac{d}{ds} w_t(s) = -w_t(s) + \sigma(D_{11} w_t(s) + b_w)$, where $b_w = C_1 x_t + D_{12} u_t + b_w$ is “frozen” for each time-step.

One interpretation of the REN model is that it represents a two-timescale or singular perturbation model, in which the “fast” dynamics in w are assumed to reach equilibrium well within each time-step of the “slow” dynamics $x_t \rightarrow x_{t+1}$.

RENs can be conveniently represented as a feedback interconnection of a linear system G and a static, memoryless nonlinear operator σ , as depicted in Fig. 1:

$$\begin{bmatrix} x_{t+1} \\ v_t \\ y_t \end{bmatrix} = \overbrace{\begin{bmatrix} A & B_1 & B_2 \\ C_1 & D_{11} & D_{12} \\ C_2 & D_{21} & D_{22} \end{bmatrix}}^W \begin{bmatrix} x_t \\ w_t \\ u_t \end{bmatrix} + \overbrace{\begin{bmatrix} b_x \\ b_w \\ b_y \end{bmatrix}}^b, \quad (8)$$

$$w_t = \sigma(v_t) := [\sigma(v_t^1) \quad \sigma(v_t^2) \quad \cdots \quad \sigma(v_t^q)]^\top, \quad (9)$$

where $v_t, w_t \in \mathbb{R}^q$ are the input and output of neurons respectively. The learnable parameters are the weight matrix $W \in \mathbb{R}^{(n+p+q) \times (n+m+q)}$, and the bias vector $b \in \mathbb{R}^{n+p+q}$. The nonlinear “activation function” σ is fixed, and for simplicity we assume the same nonlinearity is applied to each channel, although this is not essential.

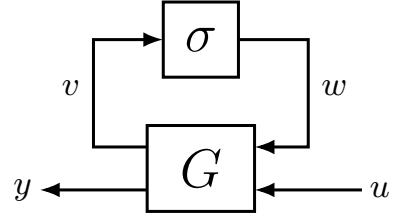


Fig. 1: REN as a feedback interconnection of a linear system G and a nonlinear activation σ .

A. Flexibility of Equilibrium Networks

The equilibrium network (7) is quite flexible as it contains many feedforward network architectures as special cases. For example, a standard L -layer deep neural network takes the form

$$\begin{aligned} z_0 &= u, \\ z_{l+1} &= \sigma(W_l z_l + b_l), \quad l = 0, \dots, L-1 \\ y &= W_L z_L + b_L \end{aligned} \quad (10)$$

where z_l is the output of the l th hidden layer. This can be written as an equilibrium network with

$$\begin{aligned} w &= \text{col}(z_1, \dots, z_L), \quad b_w = \text{col}(b_0, \dots, b_{L-1}), \quad b_y = b_L \\ D_{12} &= \text{col}(W_0, 0, \dots, 0), \quad D_{21} = \begin{bmatrix} 0 & \cdots & 0 & W_L \end{bmatrix}, \end{aligned}$$

$$D_{11} = \begin{bmatrix} 0 & & & \\ W_1 & \ddots & & \\ \vdots & \ddots & 0 & \\ 0 & \cdots & W_{L-1} & 0 \end{bmatrix}.$$

Equilibrium networks can represent many other interesting structures including residual, convolution, and other feedforward networks. The reader is referred to [59]–[61] for further details.

B. Acyclic RENs and Well-Posedness

A useful subclass of REN is the *acyclic REN* (aREN) where the weight D_{11} is constrained to be strictly lower triangular. We can interpret D_{11} as the adjacency matrix of a directed graph defining interconnections between the neurons (activation functions) in the equilibrium network. If D_{11} is strictly lower triangular then this graph is guaranteed to be acyclic. Compared to the general REN, the aREN is simpler to implement since model evaluation does not require a fixed point equation to be solved and in our experience often provides similar quality of solutions.

The general REN with full D_{11} may include many cycles. An important question then is well-posedness, i.e., a existence of a unique solution w_t^* of (7) for any input b_w . In [60] it was shown that if there exists a $\Lambda \in \mathbb{D}_+^q$ such that

$$2\Lambda - \Lambda D - D^\top \Lambda \succ 0, \quad (11)$$

then the equilibrium network is well-posed.

C. Computational Details of RENs

For a well-posed REN with full D_{11} , solutions can be computed by formulating an equivalent monotone operator splitting problem [62]. In the authors' experience, the Peaceman Rachford algorithm is reliable and efficient [60].

When training an equilibrium network via gradient descent, we need to compute the Jacobian $\partial w_t^*/\partial(\cdot)$ where w_t^* is the solution of the implicit equation (7), and (\cdot) denotes the input to the network or model parameters. By using the implicit function theorem, $\partial w_t^*/\partial(\cdot)$ can be computed via

$$\frac{\partial w_t^*}{\partial(\cdot)} = (I - JD)^{-1} J \frac{\partial(Dw_t^* + b_w)}{\partial(\cdot)} \quad (12)$$

where J is the Clarke generalized Jacobian of σ at $Dw_t^* + b_w$. From Assumption 1 in Section III-D, we have that J is a singleton almost everywhere. In particular, J is a diagonal matrix satisfying $0 \preceq J \preceq I$. The matrix $I - JD$ is invertible by Condition (11) [60].

D. Contracting and Robust RENs

We call the model of (8), (9) a contracting REN (C-REN) if it is contracting and a robust REN (R-REN) if it satisfies the incremental IQC defined by (Q, S, R) . Similarly, contracting a-REN (C-aREN) and robust a-REN (R-aREN) can be defined by imposing an additional structural constraint (i.e., D_{11} is strictly lower-triangular). Here we present the conditions for C-RENs and R-RENs based on incremental analysis.

For any two sequences $z^a = (x^a, w^a, v^a, u^a)$ and $z^b = (x^b, w^b, v^b, u^b)$ generated by (1), the dynamics of $\Delta z := z^a - z^b$ can be represented by

$$\begin{bmatrix} \Delta x_{t+1} \\ \Delta v_t \\ \Delta y_t \end{bmatrix} = \begin{bmatrix} A & B_1 & B_2 \\ C_1 & D_{11} & D_{12} \\ C_2 & D_{21} & D_{22} \end{bmatrix} \begin{bmatrix} \Delta x_t \\ \Delta w_t \\ \Delta u_t \end{bmatrix}, \quad (13)$$

$$\Delta w_t = \sigma(v_t + \Delta v_t) - \sigma(v_t). \quad (14)$$

We make the following assumption on σ , which holds for most activation functions in the literature [63].

Assumption 1: The activation function σ is piecewise differentiable and slope-restricted in $[0, 1]$, i.e.,

$$0 \leq \frac{\sigma(y) - \sigma(x)}{y - x} \leq 1, \quad \forall x, y \in \mathbb{R}, x \neq y. \quad (15)$$

By taking a conic combination of the above constraint in the i th channel with multipliers $\lambda_i > 0$, we obtain the following incremental quadratic constraint

$$\Gamma_t = \begin{bmatrix} \Delta v_t \\ \Delta w_t \end{bmatrix}^\top \begin{bmatrix} 0 & \Lambda \\ \Lambda & -2\Lambda \end{bmatrix} \begin{bmatrix} \Delta v_t \\ \Delta w_t \end{bmatrix} \geq 0, \quad \forall t \in \mathbb{N} \quad (16)$$

where $\Lambda = \text{diag}(\lambda_1, \dots, \lambda_q) \in \mathbb{D}_+$.

The following proposition gives conditions for contracting and robust RENs using the IQC framework [64].

Proposition 1: A REN in (8), (9) is contracting if there exist $P \succ 0$ and $\Lambda \in \mathbb{D}_+$ satisfying

$$\begin{bmatrix} P & -C_1^\top \Lambda \\ -\Lambda C_1 & W \end{bmatrix} - \begin{bmatrix} A^\top \\ B_1^\top \end{bmatrix} P \begin{bmatrix} A^\top \\ B_1^\top \end{bmatrix}^\top \succ 0 \quad (17)$$

where $W = 2\Lambda - \Lambda D_{11} - D_{11}^\top \Lambda$. It satisfies the incremental IQC defined by (Q, S, R) if there exist $P \succ 0$ and $\Lambda \in \mathbb{D}_+$ such that

$$\begin{bmatrix} P & -C_1^\top \Lambda & C_2^\top S^\top \\ -\Lambda C_1 & W & D_{21}^\top S^\top - \Lambda D_{12} \\ SC_2 & SD_{21} - D_{12}^\top \Lambda & R + SD_{22} + D_{22}^\top S^\top \end{bmatrix} - \begin{bmatrix} A^\top \\ B_1^\top \\ B_2^\top \end{bmatrix} P \begin{bmatrix} A^\top \\ B_1^\top \\ B_2^\top \end{bmatrix}^\top + \begin{bmatrix} C_2^\top \\ D_{21}^\top \\ D_{22}^\top \end{bmatrix} Q \begin{bmatrix} C_2^\top \\ D_{21}^\top \\ D_{22}^\top \end{bmatrix}^\top \succ 0. \quad (18)$$

The proof can be found in Appendix A.

Remark 2: It is worth pointing out that both Conditions (17) and (18) are not jointly convex in the model parameter θ , stability certificate P , and multiplier Λ .

Remark 3: If only *non-incremental* forms of stability are considered, i.e. signal boundedness rather than contraction, then we can incorporate a richer (more powerful) class of multipliers for repeated nonlinearities, as previously discussed in [65]–[67]. However, these multipliers are not valid for the incremental case since the Δw_t^i explicitly depend on the values of v_t^i which may differ among channels [60].

IV. CONVEX PARAMETERIZATIONS OF RENs

In this section we propose convex parameterizations for C-RENs/R-RENs, which are based on the following implicit representation of the linear component G :

$$\begin{bmatrix} Ex_{t+1} \\ \Lambda v_t \\ y_t \end{bmatrix} = \begin{bmatrix} F & \mathcal{B}_1 & \mathcal{B}_2 \\ C_1 & \mathcal{D}_{11} & \mathcal{D}_{12} \\ C_2 & \mathcal{D}_{21} & \mathcal{D}_{22} \end{bmatrix} \begin{bmatrix} x_t \\ w_t \\ u_t \end{bmatrix} + \tilde{b} \quad (19)$$

where E is an invertible matrix and Λ is a positive-definite diagonal matrix. Note that the explicit linear model (8) can be easily constructed from (19) by inverting E and Λ . While the parameters E and Λ do not expand the model set, the extra degrees of freedom will allow us to formulate sets of C-RENs and R-RENs that are jointly convex in the model parameter, stability certificate, and multipliers.

Definition 4: A model of the form (19), (9) is said to be well-posed if it yields a unique (w_t, x_{t+1}) for any x_t, u_t and b , and hence a unique response to any initial conditions and input.

To construct a convex parameterization of C-RENs, we introduce the following LMI constraint:

$$\begin{bmatrix} E + E^\top - \mathcal{P} & -C_1^\top & F^\top \\ -C_1 & \mathcal{W} & \mathcal{B}_1^\top \\ F & \mathcal{B}_1 & \mathcal{P} \end{bmatrix} \succ 0, \quad (20)$$

where $\mathcal{W} = 2\Lambda - \mathcal{D}_{11} - \mathcal{D}_{11}^\top$. The convex parameterization of C-RENs is then given by

$$\Theta_C := \{\theta \mid \exists \mathcal{P} \succ 0 \text{ s.t. (20)}\}.$$

To construct convex parameterization of R-RENs, we propose the following convex constraint:

$$\begin{aligned} & \begin{bmatrix} E + E^\top - \mathcal{P} & -C_1^\top & C_2^\top S^\top \\ -C_1 & \mathcal{W} & D_{21}^\top S^\top - \mathcal{D}_{12} \\ SC_2 & SD_{21} - \mathcal{D}_{12}^\top & R + SD_{22} + D_{22}^\top S^\top \end{bmatrix} \\ & - \begin{bmatrix} F^\top \\ \mathcal{B}_1^\top \\ \mathcal{B}_2^\top \end{bmatrix} \mathcal{P}^{-1} \begin{bmatrix} F^\top \\ \mathcal{B}_1^\top \\ \mathcal{B}_2^\top \end{bmatrix}^\top + \begin{bmatrix} C_2^\top \\ D_{21}^\top \\ D_{22}^\top \end{bmatrix} Q \begin{bmatrix} C_2^\top \\ D_{21}^\top \\ D_{22}^\top \end{bmatrix}^\top \succ 0 \end{aligned} \quad (21)$$

where $Q \preceq 0$, S , and R are given. The convex parameterization of R-REns is then defined as

$$\Theta_R := \{\theta \mid \exists \mathcal{P} \succ 0 \text{ s.t. (21)}\}.$$

The following result relates the above parameterizations to the desired model behavioural properties:

Theorem 1: All models in Θ_C are well-posed and contracting. All models in Θ_R are well-posed, contracting, and satisfy the IQC defined by (Q, S, R) .

Remark 4: We can modify Condition (17) to characterize C-REns with a specified contraction rate $\alpha \in [0, 1]$:

$$\begin{bmatrix} E + E^\top - \frac{1}{\alpha} \mathcal{P} & -C_1^\top & F^\top \\ -C_1 & \mathcal{W} & \mathcal{B}_1^\top \\ F & \mathcal{B}_1 & \mathcal{P} \end{bmatrix} \succ 0.$$

One can even allow $\alpha > 1$ to characterize ‘‘slowly expanding’’ networks if desired.

Remark 5: It is straightforward to enforce an acyclic property on the REN or any other sparsity structure on D_{11} e.g. corresponding to the standard feedforward network in Section III-A with specified layers. Since Λ is diagonal, the sparsity structures of \mathcal{D}_{11} and $D_{11} = \Lambda^{-1} \mathcal{D}_{11}$ are identical, and so the desired structure can be added as a convex constraint on \mathcal{D}_{11} .

The following result implies that all contracting models in our set are also Lipschitz bounded;

Theorem 2: All models in $\Theta_C \supset \Theta_R$ have a finite ℓ_2 Lipschitz bound.

The proof can be found in Appendix C, which is based showing that (21) is equivalent to

$$\mathcal{R} := R + SD_{22} + D_{22}^\top S^\top + D_{22}^\top Q D_{22} \succ 0, \quad (22a)$$

$$\begin{aligned} & \begin{bmatrix} E + E^\top - \mathcal{P} & -C_1^\top & F^\top \\ -C_1 & \mathcal{W} & \mathcal{B}_1^\top \\ F & \mathcal{B}_1 & \mathcal{P} \end{bmatrix} \succ \\ & \begin{bmatrix} C_2^\top \\ D_{21}^\top \\ \mathcal{B}_2^\top \end{bmatrix} \mathcal{R}^{-1} \begin{bmatrix} C_2^\top \\ D_{21}^\top \\ \mathcal{B}_2^\top \end{bmatrix}^\top - \begin{bmatrix} C_2^\top \\ D_{21}^\top \\ 0 \end{bmatrix} Q \begin{bmatrix} C_2^\top \\ D_{21}^\top \\ 0 \end{bmatrix}^\top, \end{aligned} \quad (22b)$$

where $\mathcal{C}_2 = (D_{22}^\top Q + S)C_2$ and $\mathcal{D}_{21} = (D_{22}^\top Q + S)D_{21} - \mathcal{D}_{12}^\top$.

V. DIRECT PARAMETERIZATIONS OF RENs

In the previous section we gave convex parameterizations of contracting and robust RENs. While convexity of a model set is useful, the conditions involved linear matrix inequalities which can be challenging to verify for large-scale models.

In this section we provide *direct* parameterizations, i.e. smooth mappings from \mathbb{R}^N to the weights and biases of contracting and robust RENs. This enables learning to be done via

unconstrained optimization, significantly enhancing the ease of use of RENs, and also enables random sampling of REN models with prescribed stability and robustness conditions.

A. Direct Parameterizations of Contracting RENs

The main idea of our construction is to notice that the matrix in the contraction LMI (20) is dense and quite simple in its relation to the model parameters, so we can in fact parameterize it directly as $X^\top X + \epsilon I$ with X a free matrix variable and ϵ a small positive constant, and from this extract the required model parameters. This idea goes back to the Burer-Monteiro method [52] for solving large-scale semidefinite programs.

To be precise, let

$$H = \begin{bmatrix} H_{11} & H_{12} & H_{13} \\ H_{21} & H_{22} & H_{23} \\ H_{31} & H_{32} & H_{33} \end{bmatrix} = X^\top X + \epsilon I \quad (23)$$

which is positive-definite by construction, where we have partitioned H into blocks of size n, n , and q . Comparing (23) to (20) we can immediately construct

$$F = H_{31}, \quad \mathcal{B}_1 = H_{32}, \quad \mathcal{P} = H_{33}, \quad C_1 = -H_{21}. \quad (24)$$

Further, it can easily be verified that the construction

$$E = \frac{1}{2}(H_{11} + \mathcal{P} + Y_1 - Y_1^\top), \quad (25)$$

where Y_1 is a free matrix variable, results in $H_{11} = E + E - \mathcal{P}$.

To obtain an aREN, we need to construct a strictly lower-triangular \mathcal{D}_{11} satisfying

$$H_{22} = \mathcal{W} = 2\Lambda - \mathcal{D}_{11} - \mathcal{D}_{11}^\top. \quad (26)$$

By taking the following matrix partition

$$H_{22} = D - L - L^\top \quad (27)$$

where D is a diagonal matrix and L is a strictly lower-triangular matrix, we have

$$\Lambda = \frac{1}{2}D, \quad \mathcal{D}_{11} = L. \quad (28)$$

Other model parameters do not affect model stability, and can be treated as free parameters.

To summarize, the parameter vector θ of a C-aREN consists of free variables: $X \in \mathbb{R}^{(2n+q) \times (2n+q)}$, $\mathcal{B}_2 \in \mathbb{R}^{n \times m}$, $C_2 \in \mathbb{R}^{p \times n}$, $\mathcal{D}_{12} \in \mathbb{R}^{q \times m}$, $D_{21} \in \mathbb{R}^{p \times q}$, $D_{22} \in \mathbb{R}^{p \times m}$ and $Y_1 \in \mathbb{R}^{n \times n}$, and model parameters are constructed via (24), (25) and (28).

The construction of a contracting REN with full (not acyclic) D_{11} is the same except that we introduce two additional free variables: $g \in \mathbb{R}^q$ and $Y_2 \in \mathbb{R}^{q \times q}$, and then construct a positive diagonal matrix $\Lambda = e^{\text{diag}(g)}$ and

$$\mathcal{D}_{11} = \Lambda - \frac{1}{2}(H_{22} + Y_2 - Y_2^\top), \quad (29)$$

which also results in (26).

B. Direct Parameterizations of Robust RENs

We now provide a direct parameterization of RENs satisfying the robustness condition (21). We have noted that this is equivalent to satisfying both (22a) and (22b) and our first step is to construct a D_{22} satisfying (22a), after which we construct the remaining model parameters satisfying (22b).

In many applications it is acceptable to have a model in which D_{22} , the direct feedthrough from input to output, is zero. In the context of LTI systems, this corresponds to a strictly proper model. In such a case (22a) reduces to $R > 0$ and the first step below can be skipped.

1) *Construction of D_{22} Satisfying (22a)*: We first define $\mathcal{Q} = Q - \epsilon I \prec 0$ where $\epsilon > 0$ as a small constant, which may be fixed or parameterized, and rewrite (22a) as

$$R + SD_{22} + D_{22}^\top S^\top + D_{22}^\top \mathcal{Q} D_{22} \succ 0 \quad (30)$$

note that ϵ can be omitted if $Q \prec 0$.

Now, the direct parameterization of D_{22} proceeds as follows: let $X_3, Y_3 \in \mathbb{R}^{s \times s}$ be the free variables, where $s = \max(p, m)$, and define

$$M = X_3^\top X_3 + Y_3 - Y_3^\top + \epsilon I. \quad (31)$$

Now set

$$Z = [(I - M)(I + M)^{-1}]_{p \times m} \quad (32)$$

where $[A]_{n \times m}$ denotes the upper-left (n, m) -block of the matrix A .

Now we construct the following factorizations:

$$L_Q^\top L_Q = -\mathcal{Q}, \quad L_R^\top L_R = R - S\mathcal{Q}^{-1}S^\top \quad (33)$$

and finally we construct D_{22} as:

$$D_{22} = -\mathcal{Q}^{-1}S^\top + L_Q^{-1}ZL_R. \quad (34)$$

and we have the following proposition:

Proposition 2: The construction of D_{22} om (31), (32), (33), (34) satisfies Condition (30).

A proof is in Appendix D.

The following are direct parameterizations of D_{22} for some important subsets of Θ_R :

- Incrementally ℓ_2 stable RENs with Lipschitz bound of γ (i.e., $Q = -\frac{1}{\gamma}I, R = \gamma I, S = 0$).
- Incrementally strictly output passive RENs (i.e., $Q = -2\rho I, R = 0, S = I$): We have $D_{22} = \frac{1}{\rho}(I + M)^{-1}$.
- Incrementally input passive RENs (i.e., $Q = 0, R = -2\nu I, S = I$): In this case, Condition (22a) becomes an LMI of the form $D_{22} + D_{22}^\top - 2\nu I \succ 0$, which yields a simple parameterization with $D_{22} = \nu I + M$.

2) *Construction of Remaining Model Parameters*: The construction of remaining parameters is similar to the contracting case above. Condition (22b) can be satisfied if we choose

$$H = X^\top X + \epsilon I +$$

$$\begin{bmatrix} C_2^\top \\ D_{21}^\top \\ \mathcal{B}_2 \end{bmatrix} \mathcal{R}^{-1} \begin{bmatrix} C_2^\top \\ D_{21}^\top \\ \mathcal{B}_2 \end{bmatrix}^\top - \begin{bmatrix} C_2^\top \\ D_{21}^\top \\ 0 \end{bmatrix} Q \begin{bmatrix} C_2^\top \\ D_{21}^\top \\ 0 \end{bmatrix}^\top \succ 0, \quad (35)$$

and then compute the model parameters of robust RENs based on the matrix partition of H in (23). A special case with $Q = -\frac{1}{\gamma}I, R = \gamma I, S = 0$ and D_{22} was reported in [57].

C. Random Sampling of Nonlinear Systems and Echo State Networks

One benefit of the direct parameterizations of RENs is that it is straightforward to randomly sample systems with the desired behavioural properties. Since contracting and robust RENs are constructed as the image of \mathbb{R}^N under a smooth mapping (Sections V-A and V-B), one can sample random vectors in \mathbb{R}^N and map them to random stable/robust nonlinear dynamical systems.

An ‘‘echo state network’’ is a state-space model with randomly sampled, but fixed, state dynamics, and a learnable output map:

$$x_{t+1} = f(x_t, u_t) \quad (36)$$

$$y_{t+1} = g(x_t, u_t, \theta) \quad (37)$$

where f is fixed and g is affinely parameterized by θ , i.e.

$$g(x_t, u_t, \theta) = g_0(x_t, u_t) + \sum_i \theta_i g^i(x_t, u_t).$$

Then, e.g. system identification with a simulation-error criteria can be solved as a basic least squares problem. This approach is reminiscent of system identification via a basis of stable linear responses (see, e.g., [68]).

For this approach to work, it is essential that the random dynamics are stable. In [55], [56] and references therein, contraction of (36) is referred to as the ‘‘echo state property’’, and simple parameterizations are given for which contraction is guaranteed.

The direct parameterizations of REN can be used to randomly sample from a rich class of contracting models, by sampling $X, Y_1, Y_2, \mathcal{B}_2, \mathcal{D}_{12}$ to construct the state-space dynamics and equilibrium network. Such a model can be used e.g. for system identification by simulating its response to inputs to generate data $\hat{u}_t, \hat{x}_t, \hat{w}_t$, and then the output mapping

$$y_t = C_2 \tilde{x}_t + D_{21} \tilde{w}_t + D_{22} \tilde{u}_t + b_y$$

can be fit to \tilde{y}_t , minimizing (3) via least-squares to obtain the parameters C_2, D_{21}, D_{22}, b_y . We will also see in Section IX how this approach can be applied in data-driven feedback control design.

VI. EXPRESSIVITY OF REN MODEL CLASS

The set of RENs contain many prior model structures as special cases. We now discuss the relationship to some prior model types:

1) *Robust and Contracting RNNs and Echo State Networks*: If we set $D_{11} = 0$, then the nonlinearity is not an equilibrium network but a single-hidden-layer neural network, and our model set Θ_C reduces to the model set proposed in [10]. Therefore, the REN model class also includes all other models that were proven to be in that model set in [10], including:

- 1) all stable linear time-invariant (LTI) systems satisfying the corresponding IQC.
- 2) all prior sets of contracting RNNs including the ciRNN [32], s-RNN [30].

We note that the stability test for the ciRNN, contraction with respect to a diagonal metric, is the same as that proposed for

echo state networks [55], [56], by randomly sampling RENs as in Section V-C we sample from a strictly larger set of echo state networks than previously known.

2) *Block Structured Models*: Block structured models are constructed from series interconnections of LTI systems and static nonlinearities [69], [70]. The REN contains block structured models as a subset, where the built-in equilibrium network can approximate any continuous static nonlinearity and the linear system represents the LTI block. For simplicity, we only consider two simple block oriented models:

- 1) *Wiener systems* consist of an LTI block followed by a static non-linearity. This structure is replicated in (8), (9) when $B_1 = 0$ and $C_2 = 0$. In this case the linear dynamical system evolves independently of the nonlinearities and feeds into a equilibrium network.
- 2) *Hammerstein systems* consist of a static non-linearity connected to an LTI system. This is represented in the REN when $B_2 = 0$ and $C_1 = 0$. In this case the input passes through a static equilibrium network and into an LTI system.

Other more complex block-oriented models such as [71] can also be constructed as RENs in a similarly straightforward manner.

3) *Nonlinear Finite Impulse Response Models*: Finite impulse response models are finite memory nonlinear filters. These have a similar construction to Wiener systems, where the LTI system contains a delay system that stores a finite history of inputs. The REN recovers a set of finite memory filters when

$$A = \begin{bmatrix} 0 & & & & \\ I & 0 & & & \\ & I & \ddots & & \\ & & & \ddots & \\ & & & & \ddots \end{bmatrix}, \quad B_2 = \begin{bmatrix} I \\ 0 \\ 0 \\ \vdots \end{bmatrix}, \quad B_1 = 0. \quad (38)$$

The output is then a nonlinear function of a truncated history of inputs.

VII. USE CASE: STABLE AND ROBUST NONLINEAR SYSTEM IDENTIFICATION

We demonstrate the proposed model set on the F16 ground vibration [72] and Wiener Hammerstein with process noise [73] system identification benchmark. We will compare the C-aREN and Lipschitz bounded R-aREN (i.e., robust REN with some prescribed Lipschitz bound of $\bar{\gamma}$, denoted by R-aREN $\gamma < \bar{\gamma}$) with an LSTM and RNN with a similar number of parameters. We will also compare to the Robust RNN proposed in [10] using the code found at [74].

An advantage of using a direct parametrization is that unconstrained optimization techniques can be applied. We fit models by minimizing simulation error:

$$\mathcal{L}_{sc}(\tilde{z}, \theta) = \|\tilde{y} - \mathfrak{R}_a(\tilde{u})\|_T^2 \quad (39)$$

using minibatch gradient descent with the Adam optimizer [53].

When training RENs, we use the Peaceman-Rachford monotone operator splitting algorithm [59], [60], [62] to solve for

the fixed points in (7). We use the conjugate gradient method to solve for the gradients with the respect to the equilibrium layer (7). The remaining gradients are calculated using the automatic differentiation tool, Zygote [75].

Model performance is measured using normalized root mean square error on the test sets, calculated as:

$$\text{NRMSE} = \frac{\|\tilde{y} - \mathfrak{R}_a(\tilde{u})\|_T}{\|\tilde{y}\|_T}. \quad (40)$$

Model robustness is measured in terms of the maximum observed sensitivity:

$$\underline{\gamma} = \max_{u,v,a} \frac{\|\mathfrak{R}_a(u) - \mathfrak{R}_a(v)\|_T}{\|u - v\|_T}. \quad (41)$$

We find a local solution to (41) using gradient ascent with the Adam optimizer. Consequently $\underline{\gamma}$ is a lower bound on the true Lipschitz constant of the sequence-to-sequence map.

A. Benchmark Datasets and Training Details

1) *F16 System Identification Benchmark*: The F16 ground vibration benchmark dataset [72] consists of accelerations measured by three accelerometers, induced in the structure of an F16 fighter jet by a wing mounted shaker. We use the multisine excitation dataset with full frequency grid. This dataset consists of 7 multisine experiments with 73,728 samples and varying amplitude. We use datasets 1, 3, 5 and 7 for training and datasets 2, 4 and 6 for testing. All test data was standardized before model fitting.

All models fit have approximately 118,000 parameters. That is, the RNN has 340 neurons, the LSTM has 170 neurons and the RENs have width $n = 75$ and $q = 150$. Models were trained for 70 epochs with a sequence length of 1024. The learning rate was initialized at 10^{-3} and was reduced by a factor of 10 every 20 Epochs.

2) *Wiener-Hammerstein With Process Noise Benchmark*: The Wiener Hammerstein with process noise benchmark dataset [76] involves the estimation of the output voltage from two input voltage measurements for a block oriented Wiener-Hammerstein system with large process noise that complicates model fitting. We have used the Multi-sine fade-out dataset consisting of two realisations of a multi-sine input signal with 8192 samples each. The test set consists of two experiments, a random phase multi-sine and a sine sweep, conducted without the added process noise.

All models fit have approximately 42,000 parameters. That is, the RNN has 200 neurons, the LSTM has 100 neurons and the RENs have $n = 40$ and $q = 100$. Models were trained for 60 epochs with a sequence length of 512. The initial learning rate was 1×10^{-3} . After 40 epochs, the learning rate was reduced to 1×10^{-4} .

B. Results and Discussion

We have plotted the mean test performance versus the observed sensitivity of the models trained on the F16 and Wiener-Hammerstein Benchmarks in Fig. 2 and 3, respectively. The dashed vertical lines show the guaranteed upper bounds on the Lipschitz constant for the RENs. In all cases,

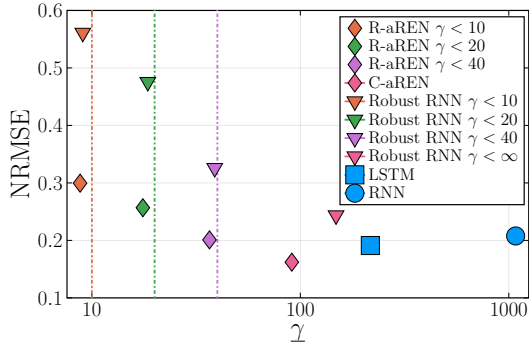


Fig. 2: Nominal performance versus robustness for models trained on F16 ground vibration benchmark dataset. The dashed vertical lines are the guaranteed upper bounds on γ corresponding to the models with matching color.

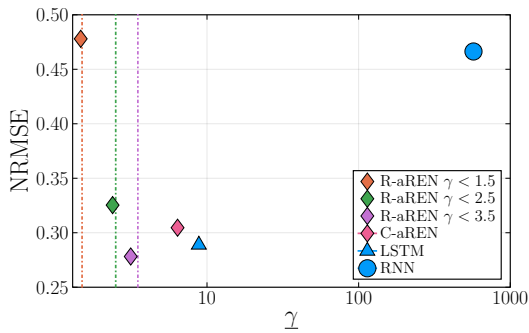


Fig. 3: Nominal performance versus robustness for models trained on Wiener-Hammerstein with process noise benchmark dataset. The dashed vertical lines are the guaranteed upper bounds on γ corresponding to the models with matching color.

we observe that the REN provides the best trade-off between nominal performance and robustness, with the REN slightly outperforming the LSTM in terms of nominal test error for large γ . By tuning γ , nominal test performance can be traded-off for robustness, signified by the consistent trend moving diagonally up and left with decreasing γ . In all cases, we found that the REN was significantly more robust than the RNN, typically having about 10% of the sensitivity for the F16 benchmark and 1% on the Wiener-Hammerstein benchmark. Also note that for small γ , the observed lower bound on the Lipschitz constant is very close to the guaranteed upper bound, showing that the real Lipschitz constant of the models is close to the upper bound.

Compared to the robust RNN proposed in [10], the REN has similar bounds on the incremental ℓ_2 gain, however the added flexibility from the term D_{11} significantly improves the nominal model performance for a given gain bound. Additionally, while both the C-aREN and Robust RNN $\gamma < \infty$ are contracting models, we note that the C-aREN is significantly more expressive with a NRMSE of 0.16 versus 0.24.

It is well known that many neural networks are very sensitive to adversarial perturbations. This is shown, for instance, in Fig. 4 and 5, where we have plotted the change in output for a small adversarial perturbation $\|\Delta u\| < 0.05$, for a selection of

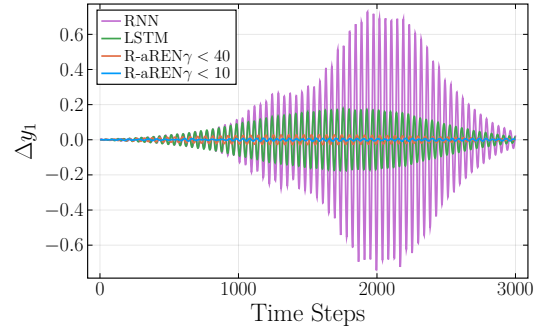


Fig. 4: Change in output of models subject to an adversarial perturbation of $\|\Delta u\| < 0.05$. The incremental gains from Δu to Δy are 980, 290, 37 and 8.6 respectively.

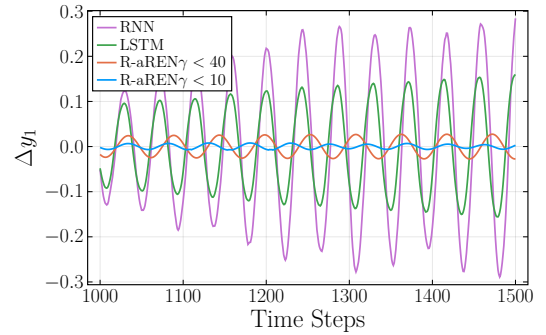


Fig. 5: Zoomed in version of Fig. 4.

models trained on the F16 benchmark dataset. Here, we can see that both the RNN and LSTM are very sensitive to the input perturbation. The R-aREN on the hand, has guaranteed bounds on the effect of the perturbation and is significantly more robust.

We have also trained R-RENs and C-RENs for the F16 and Wiener Hammerstein Benchmark datasets. The resulting nominal performance and sensitivities for the aRENs and RENs are shown in Table I. We do not observe a significant difference in performance between the cyclic and acyclic model classes.

Finally, we have plotted the loss versus the number of

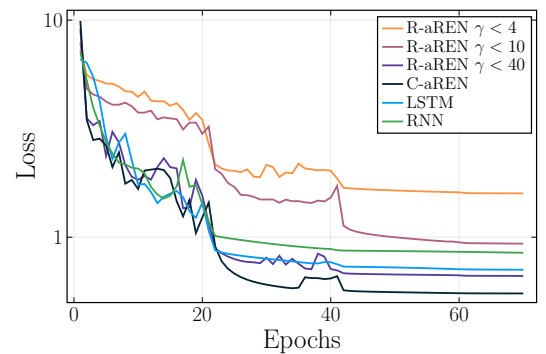


Fig. 6: Nominal performance versus robustness for models trained on F16 ground vibration benchmark dataset.

TABLE I: Upper and lower bounds on incremental ℓ_2 gain and nominal performance for aREN and REN.

	$\bar{\gamma}$	10	20	40	60	100	∞
aREN	$\underline{\gamma}$	8.8	17.5	36.7	44.9	60.56	91.0
	NRMSE (%)	30.0	25.7	20.1	18.5	17.2	16.2
REN	$\underline{\gamma}$	9.1	17.1	36.0	44.6	57.9	85.26
	NRMSE (%)	30.3	26.8	21.8	19.9	19.3	16.8

epochs in Fig. 6 for some of the models on the F16 dataset. Compared to the LSTM, the REN takes a similar number of steps and achieves a slightly lower training loss. The LSTM is a model designed to be easy to train.

VIII. USE CASE: LEARNING NONLINEAR OBSERVERS

Estimation of system states from incomplete and/or noisy measurements is an important problem in many practical applications. For linear systems with Gaussian noise, a simple and optimal solution exists in the form of the Kalman filter, but for nonlinear systems even achieving estimation stability is non-trivial and many approaches have been investigated, e.g. [77]–[79]. State estimation a.k.a. observer design was one of the original motivations for contraction analysis [12], and in this section, we show how a flexible set of contracting models can be used to learn stable state observers via *snapshots* of a nonlinear system model.

Given a nonlinear system of the form

$$x_{t+1} = f_m(x_t, u_t, w_t), \quad y_t = g_m(x_t, u_t, w_t) \quad (42)$$

where $x_t \in \mathbb{X}$ is an internal state to be estimated, y_t is an available measurement, $u_t \in \mathbb{U}$ is a known (e.g. control) input, and w_t comprises unknown disturbances and sensor noise. Here \mathbb{X}, \mathbb{U} are some compact sets. We consider $w_t = 0$ to represent a nominal deterministic model.

A standard structure, pioneered by Luenberger, is an observer of the form

$$\hat{x}_{t+1} = f_m(\hat{x}_t, u_t, 0) + l(\hat{x}_t, u_t, y_t) \quad (43)$$

i.e. a combination of a model prediction f_m and a measurement correction function l . A common special case is $l(\hat{x}_t, u_t, y_t) = L(\hat{x})(y_t - g_m(\hat{x}_t, u_t, 0))$ for some gain $L(\hat{x})$.

In many practical cases the best available model f_m, g_m is highly complex, e.g. based on finite element methods or algorithmic mechanics [80]. This poses two major challenges to the standard paradigm:

- 1) How to design the function l such that the observer (43) is stable (preferably globally) and exhibits good noise/disturbance rejection.
- 2) The model itself may be so complex that evaluating $f_m(\hat{x}_t, u_t, 0)$ in real-time is infeasible, e.g. for stiff systems where short sample times are required.

Our parameterization of contracting models enables an alternative paradigm, first suggested for the restricted case of polynomial models in [43].

Proposition 3: If we construct an observer of the form

$$\hat{x}_{t+1} = f_o(\hat{x}_t, u_t, y_t) \quad (44)$$

such that the following two conditions hold:

- 1) The system (44) is contracting with rate $\alpha \in (0, 1)$ for some constant metric $P > 0$.
- 2) The following ‘‘correctness’’ condition holds:

$$f_m(x, u, 0) = f_o(x, u, g_m(x, u, 0)), \quad \forall (x, u) \in \mathbb{X} \times \mathbb{U}. \quad (45)$$

Then when $w = 0$ we have $\hat{x}_t \rightarrow x_t$ as $t \rightarrow \infty$. Suppose that the observer (44) satisfies Conditions 1) and

- 3) The following error bound holds:

$$|e(x, u)| \leq \rho, \quad \forall (x, u) \in \mathbb{X} \times \mathbb{U}, \quad (46)$$

$$\text{where } e(x, u) := f_o(x, u, g_m(x, u, 0)) - f_m(x, u, 0).$$

Then when $w = 0$ we have

$$|\hat{x}_t - x_t| \leq \frac{2\rho}{1-\alpha} \sqrt{\frac{\bar{\sigma}(P)}{\underline{\sigma}(P)}}, \quad \forall t \geq T \quad (47)$$

for some sufficiently large $T \in \mathbb{N}$, where $\bar{\sigma}(P)$ and $\underline{\sigma}(P)$ denote the maximum and minimum singular values of P , respectively.

The reasoning is simple: (45) implies that if $\hat{x}_0 = x_0$ then $\hat{x}_t = x_t$ for all $t \geq 0$, i.e. the true state is a particular solution of the observer. But contraction implies that all solutions of the observer converge to each other. Hence all solutions of the observer converge to the true state. The proof of the estimation error bound can be found in Appendix E.

In this paper we propose designing such observers as a supervised learning problem over our class of contracting models.

- 1) Sample a dataset $\tilde{z} = \{x^i, u^i, i = 1, 2, \dots, N\}$ where $(x^i, u^i) \in \mathbb{X} \times \mathbb{U}$.
- 2) Compute $g_m^i = g_m(x^i, u^i, 0)$ and $f_m^i = f_m(x^i, u^i, 0)$ for each i .
- 3) Learn a contracting system f_o minimizing the loss function

$$\mathcal{L}_o(\tilde{z}, \theta) = \sum_{i=1}^N |f_m^i - f_o(x^i, u^i, g_m^i)|^2 \quad (48)$$

Remark 6: An observer of traditional form (43) with $l(\hat{x}_t, u_t, y_t) = L(\hat{x})(y_t - g_m(\hat{x}_t, u_t, 0))$ will always satisfy the correctness condition, but designing $L(\hat{x})$ to achieve global convergence may be difficult. In contrast, an observer design using the proposed procedure will always achieve global convergence, but may not achieve correctness exactly. If the dataset is sufficiently dense, and the loss (48) can be driven near zero, then we can establish the estimation error bound based on Proposition 3 and the generalization bound of the observer learning problem.

A. Example: Reaction-Diffusion PDE

We illustrate this approach by designing an observer for the following semi-linear reaction-diffusion partial differential equation:

$$\frac{\partial \xi(z, t)}{\partial t} = \frac{\partial^2 \xi(z, t)}{\partial z^2} + R(\xi, z, t), \quad (49)$$

$$\xi(z, 0) = 1, \quad \xi(1, t) = \xi(0, t) = b(t) \quad (50)$$

$$y = g(\xi, z, t) \quad (51)$$

where, the state $\xi(z, t)$ is a function of both the spatial coordinate $z \in [0, 1]$ and time $t \in \mathbb{R}_+$. Models of the form (49) model processes such as combustion [81], bioreactors [82] or neural spiking dynamics [81]. The observer design problem for such systems has been considered using complex backstepping methods that guarantee only local stability [82].

We consider the case where the local reaction dynamics are have the following form, which appears in models of combustion processes [81]:

$$R(\xi, z, t) = \frac{1}{2}\xi(1 - \xi)(\xi - \frac{1}{2}).$$

We consider the boundary condition $b(t)$ as a known input and assume that there is a single measurement taken from the center of the spatial domain so $y(t) = \xi(0.5, t)$.

We discretize z into N intervals z^1, \dots, z^N where $z^i = (i - 1)\Delta z$. The state at spatial coordinate z^i and time t is then described by $\bar{\xi}_t = (\xi_t^1, \xi_t^2, \dots, \xi_t^N)$ where $\xi_t^i = \xi(z^i, t)$. The dynamics over a time period Δt can then be approximated using the following finite differences:

$$\frac{\partial \xi(z, t)}{\partial t} \approx \frac{\xi_{t+\Delta t}^i - \xi_t^i}{\Delta t}, \quad (52)$$

$$\frac{\partial^2 \xi(z, t)}{\partial z^2} \approx \frac{\xi_t^{i+1} + \xi_t^{i-1} - 2\xi_t^i}{\Delta z^2}. \quad (53)$$

Substituting (52) and (53) into (49) and rearranging for $\bar{\xi}_{t+\Delta t}$ leads to an N dimensional state space model of the form:

$$\bar{\xi}_{t+\Delta t} = a_{rd}(\bar{\xi}_t, b_t) \quad (54)$$

$$y_t = c_{rd}(\bar{\xi}_t) \quad (55)$$

We generate training data by simulating the system (54), (55) with $N = 51$ for 10^5 time steps with the stochastic input $b_{t+1} = b_t + 0.05\omega_t$ where $\omega_t \sim \mathcal{N}[0, 1]$. We denote this training data by $\tilde{z} = (\tilde{\xi}_t, \tilde{y}_t, \tilde{b}_t)$ for $t = 0, \dots, 10^5 \Delta t$.

To train an observer for this system, we construct a C-aREN with $n = 51$ and $q = 200$. We optimize the one step ahead prediction error:

$$\mathcal{L}(\tilde{z}, \theta) = \frac{1}{T} \sum_{t=0}^{T-1} |a(\tilde{\xi}_t, \tilde{b}_t) - f_o(\tilde{\xi}_t, \tilde{b}_t, \tilde{y}_t)|^2,$$

using stochastic gradient descent with the Adam optimizer [53]. Here, $f_o(\xi, b, y)$ is a C-aREN described by (8), (9) using direct parametrization discussed in Section V-A. Note that we have taken the output mapping in (8) to be $[C_2, D_{21}, D_{22}] = [I, 0, 0]$.

We have plotted results of the PDE simulation and the observer state estimates in Fig. 7. The simulation starts with an initial state of $\xi(z, 0) = 1$ and the observer has an initial state estimate of $\bar{\xi}_0 = 0$. The error between the state estimate and the PDE simulation's state quickly decays to zero and the observer state continues to track the PDE's state.

We have also provided a comparison to a free run simulation of the PDE with initial condition $\xi(z, 0) = 0$ in Fig. 8 and 9. Here we can see that simulated trajectories with different initial conditions do not converge. This suggests that the system is not contracting and the state cannot be estimated by simply running a parallel simulation. The state estimates of the observer, however, quickly converge on the true model state.

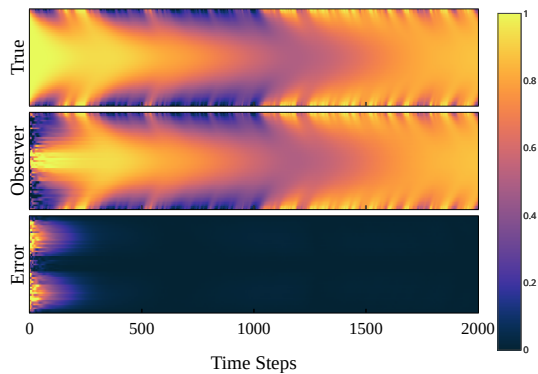
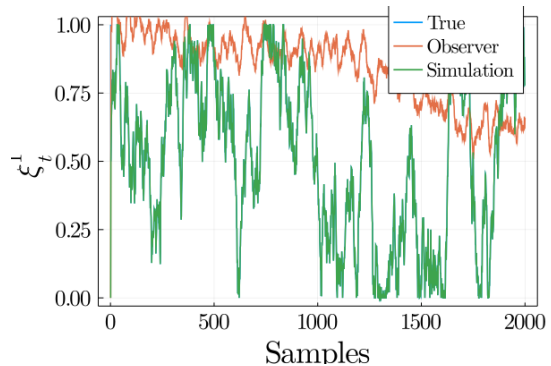
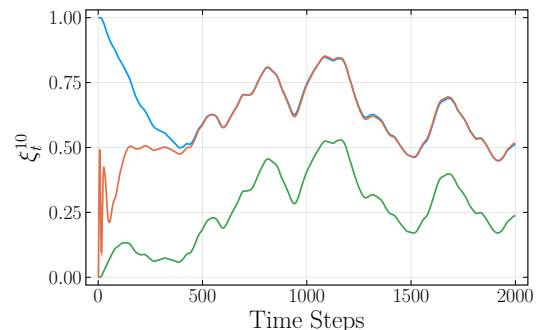


Fig. 7: Simulation of a semi-linear reaction diffusion equation and the observer's state estimate, with a measurement in the centre of the spatial domain. The y -axis corresponds to the spatial dimension and the x -axis corresponds to the time dimension.



(a) True and estimated states for ξ_t^1 , located at PDE boundary.



(b) True and estimated states for ξ_t^{10} .

Fig. 8: True state and state estimates from the designed observer and a free run simulation of the PDE.

IX. USE CASE: DATA-DRIVEN FEEDBACK CONTROL DESIGN

In this section we show how a rich class of contracting nonlinear models can be useful for nonlinear feedback design for *linear* dynamical systems with stability guarantees. Even if the dynamics are linear, the presence of constraints, non-quadratic costs, and non-Gaussian disturbance can mean that non-linear policies are superior to linear policies. Indeed, in the presence of constraints, model predictive control is a common solution.

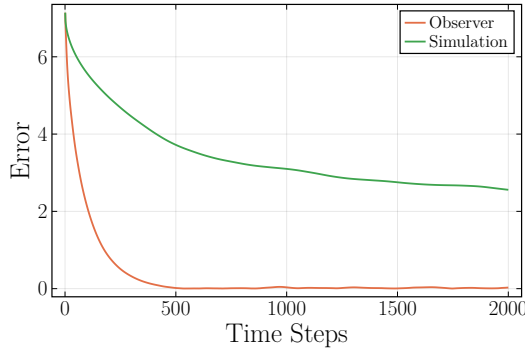


Fig. 9: State estimation error for the nonlinear observer compared to a free run simulation from the same initial conditions.

The basic idea we illustrate in this section is to build on a standard method for *linear* feedback optimization: the Youla-Kucera parameterization, a.k.a Q-augmentation [16], [83]. For a linear system model

$$x_{t+1} = \mathbb{A}x_t + \mathbb{B}_1w_t + \mathbb{B}_2u_t, \quad (56)$$

$$\zeta_t = \mathbb{C}_1x_t + \mathbb{D}_{11}w_t + \mathbb{D}_{12}u_t. \quad (57)$$

$$y_t = \mathbb{C}_2x_t + \mathbb{D}_{21}w_t. \quad (58)$$

with x the state, u the controlled input, w_t external inputs (reference, disturbance, measurement noise), y a measured output, and ζ comprises the “performance” outputs to kept small (e.g. tracking error, control signal). We assume the system is detectable and stabilizable, i.e. there exist \mathbb{L} and \mathbb{K} such that $\mathbb{A} - \mathbb{L}\mathbb{C}$ and $\mathbb{A} - \mathbb{B}\mathbb{K}$ are Schur stable. Note that if \mathbb{A} is stable we can take $\mathbb{L} = 0, \mathbb{K} = 0$. Consider a feedback controller of the form:

$$\hat{x}_{t+1} = \mathbb{A}\hat{x}_t + \mathbb{B}_2u_t + \mathbb{L}\tilde{y} \quad (59)$$

$$\tilde{y}_t = y_t - \mathbb{C}_2\hat{x}_t \quad (60)$$

$$u_t = -\mathbb{K}\hat{x}_t + v_t \quad (61)$$

i.e. a standard output-feedback structure with v_t an additional control augmentation. The closed-loop input-output dynamics can be written as the transfer matrix

$$\begin{bmatrix} \zeta \\ \tilde{y} \end{bmatrix} = \begin{bmatrix} P_{\zeta w} & P_{\zeta v} \\ P_{\tilde{y} w} & 0 \end{bmatrix} \begin{bmatrix} w \\ v \end{bmatrix} \quad (62)$$

where we have used the fact that v maps to x and \hat{x} equally, as the mapping from v to \tilde{y} is zero.

It is well-known that the set of all stabilizing linear feedback controllers can be parameterised by stable linear systems $Q : \tilde{y} \mapsto v$, and moreover this convexifies the closed-loop dynamics. A standard approach (e.g. [45]) is to construct an affine parameterization for Q via a finite-dimensional truncation of a complete basis of stable linear systems, and optimize to meet various criteria on frequency response, impulse response, and response to application-dependent test inputs.

However, if the control augmentation v is instead generated by a contracting nonlinear system $v = Q(\tilde{y})$, then the closed-loop dynamics $w \mapsto \zeta$ are nonlinear but contracting and have the representation

$$\zeta = P_{zw}w + P_{zv}Q(P_{\tilde{y}w}w). \quad (63)$$

This presents opportunities for learning stabilizing controllers via parameterizations of stable nonlinear models.

A. Echo State Network and Convex Optimization

Here we describe a particular setting in which the data-driven optimization of nonlinear policies can be posed as a *convex* problem. Suppose we wish to design a causal feedback controller solving (at least approximately) a problem of the form:

$$\min_{\theta} J(\zeta) \quad (64)$$

$$\text{s.t. } c(\zeta) \leq 0 \quad (65)$$

where ζ is the response of the performance outputs to a *particular class* of inputs w , J is a convex objective function, and c is a set of convex constraints, e.g. state and control signal bounds.

If we take Q as an echo state network, c.f. Section V-C:

$$\begin{aligned} q_{t+1} &= f_q(q_t, \tilde{y}_t) \\ v_t &= g_q(q_t, \tilde{y}_t, \theta) \end{aligned}$$

where f_q is fixed and g_q is linearly parameterized by θ , i.e.

$$g_q(q_t, \tilde{y}_t, \theta) = \sum_i \theta_i g_q^i(q_t, \tilde{y}_t).$$

Then Q has the representation

$$Q(\tilde{y}) = \sum_i \theta_i Q^i(\tilde{y})$$

where Q^i is a state-space model with dynamics f_q and output g_q^i . Then, we can perform data-driven controller optimization in the following way:

- 1) Construct (e.g. via random sampling, experiment) a finite set of test signals w^j .
- 2) Compute $\tilde{y}_t^j = P_{\tilde{y}w}w^j$ for each j .
- 3) For each j , compute the response to \tilde{y}^j :

$$q_{t+1} = f_q(q_t, \tilde{y}_t^j), \quad v_t^{ij} = g_q^i(q_t, \tilde{y}_t^j).$$

- 4) Construct the affine representation

$$\zeta^j = P_{zw}w^j + \sum_i \theta P_{zv}v^{ij}.$$

- 5) Solve the convex optimization problem:

$$\begin{aligned} \theta^* &= \arg \min_{\theta} J(\zeta) + R(\theta) \\ \text{s.t. } &c(\zeta^j) \leq 0 \end{aligned}$$

where $R(\theta)$ is an optional regularization term.

The result will of course only be approximately optimal, since w^j are but a representative sample and the echo state network provides only a finite-dimensional span of policies. However it will be *guaranteed* to be stabilizing.

Remark 7: This framework can be extended to parameterizing robustly stabilizing controllers [16] and stabilizing controllers for nonlinear systems [17], and adaptive control via online convex optimization, e.g. [84], [85] use the Youla parameterization with Q parameterized via its impulse response.

form in Δx_t , it follows that $V_{t+1} \leq \alpha V_t$ for some $\alpha \in [0, 1)$ and $V_t \leq \alpha^t V_0$.

Similarly, from (18) we can prove that the following incremental dissipation inequality holds for (13), (14):

$$V_{t+1} - V_t - \begin{bmatrix} \Delta y_t \\ \Delta u_t \end{bmatrix}^\top \begin{bmatrix} Q & S \\ S^\top & R \end{bmatrix} \begin{bmatrix} \Delta y_t \\ \Delta u_t \end{bmatrix} < \Gamma_t \leq 0. \quad (67)$$

B. Proof of Theorem 1

To show well-posedness, from (20) we have $E + E^\top \succ P \succ 0$ and $\mathcal{W} = 2\Lambda - \Lambda\Lambda^{-1}\mathcal{D}_{11} - \mathcal{D}_{11}^\top\Lambda^{-1}\Lambda \succ 0$. The first LMI implies that E is invertible [87] and thus (8) is well-posed. The second one ensures that the equilibrium network (7) is well-posed by the main result of [60].

To prove contraction, applying the inequality $E^\top \mathcal{P}^{-1} E \succeq E + E^\top - P$ and Schur complement to (20) gives

$$\begin{bmatrix} E^\top \mathcal{P}^{-1} E & -C_1^\top \\ -C_1 & \mathcal{W} \end{bmatrix} - \begin{bmatrix} F^\top \\ \mathcal{B}_1^\top \end{bmatrix} \mathcal{P}^{-1} \begin{bmatrix} F^\top \\ \mathcal{B}_1^\top \end{bmatrix}^\top \succ 0.$$

By substituting $F = EA$, $\mathcal{B}_1 = EB_1$, $\mathcal{B}_2 = EB_2$, $C_1 = \Lambda C_1$ and $\mathcal{D}_{11} = \Lambda D_{11}$ into the above inequality, we obtain (17) with $P = E^\top \mathcal{P}^{-1} E$. Thus, Θ_C is a set of C-RENs.

Similarly, we can show that (21) implies (18), i.e., Θ_R is a set of R-RENs.

C. Proof of Theorem 2

We first show that $\Theta_R \subset \Theta_C$. Applying Schur complement to (21) yields

$$\begin{bmatrix} E + E^\top - \mathcal{P} & -C_1^\top & C_2^\top & F^\top \\ -C_1 & \mathcal{W} & \mathcal{D}_{21}^\top & \mathcal{B}_1^\top \\ C_2 & \mathcal{D}_{12} & \mathcal{R} & \mathcal{B}_2^\top \\ F & \mathcal{B}_1 & \mathcal{B}_2 & \mathcal{P} \end{bmatrix} \succ - \begin{bmatrix} C_2^\top \\ \mathcal{D}_{21}^\top \\ 0 \\ 0 \end{bmatrix} Q \begin{bmatrix} C_2^\top \\ \mathcal{D}_{21}^\top \\ 0 \\ 0 \end{bmatrix}^\top.$$

By swapping the last two rows and columns for the above inequality, and then applying Schur complement to the component \mathcal{R} , we obtain Inequality (22). Then, Condition (20) follows by the facts $\mathcal{R} \succ 0$ and $Q \preceq 0$.

Now we show that any REN in Θ_C has a finite ℓ_2 Lipschitz bound. That is, Condition (20) implies that there exists a sufficiently large but finite γ such that (22) holds for $Q = -\frac{1}{\gamma}I$, $R = \gamma I$, $S = 0$, i.e.,

$$\begin{bmatrix} E + E^\top - \mathcal{P} & -C_1^\top & F^\top \\ -C_1 & \mathcal{W} & \mathcal{B}_1^\top \\ F & \mathcal{B}_1 & \mathcal{P} \end{bmatrix} \succ \Phi_\gamma \quad (68)$$

where

$$\Phi_\gamma = \frac{1}{\gamma} \begin{bmatrix} C_2^\top \\ \mathcal{D}_{21}^\top \\ 0 \end{bmatrix} \begin{bmatrix} C_2^\top \\ \mathcal{D}_{21}^\top \\ 0 \end{bmatrix}^\top + \begin{bmatrix} -\frac{1}{\gamma} C_2^\top D_{22} \\ -\frac{1}{\gamma} D_{21}^\top D_{22} - \mathcal{D}_{12} \\ \mathcal{B}_2 \end{bmatrix} \left(\gamma I - \frac{1}{\gamma} D_{22}^\top D_{22} \right)^{-1} \begin{bmatrix} -\frac{1}{\gamma} C_2^\top D_{22} \\ -\frac{1}{\gamma} D_{21}^\top D_{22} - \mathcal{D}_{12} \\ \mathcal{B}_2 \end{bmatrix}^\top.$$

For sufficiently large γ , we have

$$\Phi_\gamma \approx \frac{1}{\gamma} \left(\begin{bmatrix} C_2^\top \\ \mathcal{D}_{21}^\top \\ 0 \end{bmatrix} \begin{bmatrix} C_2^\top \\ \mathcal{D}_{21}^\top \\ 0 \end{bmatrix}^\top + \begin{bmatrix} 0 \\ -\mathcal{D}_{12} \\ \mathcal{B}_2 \end{bmatrix} \begin{bmatrix} 0 \\ -\mathcal{D}_{12} \\ \mathcal{B}_2 \end{bmatrix}^\top \right),$$

which is a positive-semidefinite matrix with arbitrary small spectral radius. Thus, for any model in Θ_C , Condition (68) holds for some sufficiently large but finite gain bound γ .

D. Proof of Proposition 2

By construction $M + M^\top \succ 0$, so we have

$$I - Z^\top Z \succ 0,$$

by the properties of the Cayley transform. Then by direct substitution, D_{22} as constructed in (34) satisfies

$$R - SQ^{-1}S^\top \succ (L_Q D_{22} - L_Q^{-\top} S^\top)^\top (L_Q D_{22} - L_Q^{-\top} S^\top),$$

which can rearranged as (30) via the factorizations (33).

E. Proof of Proposition 3

When the correctness condition (45) holds, we have that $\hat{x}_t = x_t$ for all $t \geq 0$ if $\hat{x}_0 = x_0$, i.e. the true state trajectory is a particular solution of the observer. But contraction implies that all solutions of the observer converge to each other. Hence when $w = 0$ we have $\hat{x}_t \rightarrow x_t$ as $t \rightarrow \infty$.

Now we consider the case where the correctness condition does not hold but its error is bounded, i.e., $|e(x, u)| \leq \rho$. The dynamics of $\Delta x := \hat{x} - x$ can be written as

$$\begin{aligned} \Delta x_{t+1} &= f_o(\hat{x}_t, u_t, y_t) - f_m(x_t, u_t) \\ &= F(x_t, u_t) \Delta x_t + e_t \end{aligned}$$

where $F(x_t, u_t) \Delta x_t := f_o(x_t + \Delta x_t, u_t, y_t) - f_o(x_t, u_t, y_t)$ and $e_t := e(x_t, u_t)$. Letting $V_t := \Delta x_t^\top P \Delta x_t$, we have

$$\begin{aligned} V_{t+1} - V_t &= 2e_t^\top P \Delta x_t + \Delta x_t^\top F^\top P F \Delta x_t - \Delta x_t^\top P \Delta x_t \\ &\leq 2e_t^\top P \Delta x_t - (1 - \alpha) \Delta x_t^\top P \Delta x_t. \end{aligned}$$

The above inequality is based on $F^\top P F - \alpha P \preceq 0$ (i.e., contraction). When $t \geq T$ with T sufficiently large, the estimation error satisfies $2e_t^\top P \Delta x_t - (1 - \alpha) \Delta x_t^\top P \Delta x_t \geq 0$, which gives the bound in (47).

REFERENCES

- [1] Y. LeCun, Y. Bengio, and G. Hinton, "Deep learning," *Nature*, vol. 521, no. 7553, pp. 436–444, 2015.
- [2] H. Yin, P. Seiler, M. Jin, and M. Arcaç, "Imitation learning with stability and safety guarantees," *IEEE Control Systems Letters*, 2021.
- [3] S. Levine, C. Finn, T. Darrell, and P. Abbeel, "End-to-end training of deep visuomotor policies," *The Journal of Machine Learning Research*, vol. 17, no. 1, pp. 1334–1373, 2016.
- [4] S. Dean, N. Matni, B. Recht, and V. Ye, "Robust guarantees for perception-based control," in *Learning for Dynamics and Control*. PMLR, 2020, pp. 350–360.
- [5] C. Szegedy, W. Zaremba, I. Sutskever, J. Bruna, D. Erhan, I. Goodfellow, and R. Fergus, "Intriguing properties of neural networks," *arXiv preprint arXiv:1312.6199*, 2013.
- [6] A. Russo and A. Proutiere, "Optimal Attacks on Reinforcement Learning Policies," *arXiv:1907.13548 [cs, stat]*, Jul. 2019.
- [7] V. Tjeng, K. Y. Xiao, and R. Tedrake, "Evaluating Robustness of Neural Networks with Mixed Integer Programming," in *International Conference on Learning Representations*, Sep. 2018.
- [8] A. Raghunathan, J. Steinhardt, and P. Liang, "Certified Defenses against Adversarial Examples," in *International Conference on Learning Representations*, 2018.
- [9] M. Fazlyab, A. Robey, H. Hassani, M. Morari, and G. J. Pappas, "Efficient and accurate estimation of lipschitz constants for deep neural networks." in *NeurIPS*, 2019.

- [10] M. Revay, R. Wang, and I. R. Manchester, "A convex parameterization of robust recurrent neural networks," *IEEE Control Systems Letters*, vol. 5, no. 4, pp. 1363–1368, 2021.
- [11] P. Pauli, A. Koch, J. Berberich, P. Kohler, and F. Allgower, "Training robust neural networks using Lipschitz bounds," *IEEE Control Systems Letters*, 2021.
- [12] W. Lohmiller and J.-J. E. Slotine, "On contraction analysis for non-linear systems," *Automatica*, vol. 34, pp. 683–696, 1998.
- [13] A. Megretski and A. Rantzer, "System analysis via integral quadratic constraints," *IEEE Transactions on Automatic Control*, vol. 42, no. 6, pp. 819–830, 1997.
- [14] T. Hatanaka, N. Chopra, M. Fujita, and M. W. Spong, *Passivity-based control and estimation in networked robotics*. Springer, 2015.
- [15] M. Arcak, C. Meissen, and A. Packard, *Networks of dissipative systems: compositional certification of stability, performance, and safety*. Springer, 2016.
- [16] K. Zhou, J. C. Doyle, K. Glover *et al.*, *Robust and Optimal Control*. Prentice hall New Jersey, 1996, vol. 40.
- [17] A. van der Schaft, *L₂-Gain and Passivity in Nonlinear Control*, 3rd ed. Springer-Verlag, 2017.
- [18] J. M. Maciejowski, "Guaranteed stability with subspace methods," *Systems & Control Letters*, vol. 26, no. 2, pp. 153–156, Sep. 1995.
- [19] T. Van Gestel, J. A. Suykens, P. Van Dooren, and B. De Moor, "Identification of stable models in subspace identification by using regularization," *IEEE Transactions on Automatic Control*, vol. 46, no. 9, pp. 1416–1420, 2001.
- [20] S. L. Lacy and D. S. Bernstein, "Subspace identification with guaranteed stability using constrained optimization," *IEEE Transactions on automatic control*, vol. 48, no. 7, pp. 1259–1263, 2003.
- [21] U. Nallasivam, B. Srinivasan, V. Kuppuraj, M. N. Karim, and R. Rengaswamy, "Computationally Efficient Identification of Global ARX Parameters With Guaranteed Stability," *IEEE Transactions on Automatic Control*, vol. 56, no. 6, pp. 1406–1411, Jun. 2011.
- [22] D. N. Miller and R. A. De Callafon, "Subspace identification with eigenvalue constraints," *Automatica*, vol. 49, no. 8, pp. 2468–2473, 2013.
- [23] J. Umenberger and I. R. Manchester, "Convex Bounds for Equation Error in Stable Nonlinear Identification," *IEEE Control Systems Letters*, vol. 3, no. 1, pp. 73–78, Jan. 2019.
- [24] G. Y. Mamakoukas, O. Xherija, and T. Murphey, "Memory-Efficient Learning of Stable Linear Dynamical Systems for Prediction and Control," *Advances in Neural Information Processing Systems*, vol. 33, pp. 13 527–13 538, 2020.
- [25] M. M. Tobenkin, I. R. Manchester, J. Wang, A. Megretski, and R. Tedrake, "Convex optimization in identification of stable non-linear state space models," in *49th IEEE Conference on Decision and Control (CDC)*. IEEE, 2010.
- [26] M. M. Tobenkin, I. R. Manchester, and A. Megretski, "Convex Parameterizations and Fidelity Bounds for Nonlinear Identification and Reduced-Order Modelling," *IEEE Transactions on Automatic Control*, vol. 62, no. 7, pp. 3679–3686, Jul. 2017.
- [27] J. Umenberger, J. Wagberg, I. R. Manchester, and T. B. Schön, "Maximum likelihood identification of stable linear dynamical systems," *Automatica*, vol. 96, pp. 280–292, 2018.
- [28] J. Umenberger and I. R. Manchester, "Specialized Interior-Point Algorithm for Stable Nonlinear System Identification," *IEEE Transactions on Automatic Control*, vol. 64, no. 6, pp. 2442–2456, 2018.
- [29] S. M. Khansari-Zadeh and A. Billard, "Learning Stable Nonlinear Dynamical Systems With Gaussian Mixture Models," *IEEE Transactions on Robotics*, vol. 27, no. 5, pp. 943–957, Oct. 2011.
- [30] J. Miller and M. Hardt, "Stable recurrent models," in *International Conference on Learning Representations*, 2019.
- [31] G. Manek and J. Z. Kolter, "Learning stable deep dynamics models," in *Advances in Neural Information Processing Systems*, vol. 32, 2019.
- [32] M. Revay and I. Manchester, "Contracting implicit recurrent neural networks: Stable models with improved trainability," in *Learning for Dynamics and Control*. PMLR, 2020, pp. 393–403.
- [33] M. Cheng, J. Yi, P.-Y. Chen, H. Zhang, and C.-J. Hsieh, "Seq2sick: Evaluating the robustness of sequence-to-sequence models with adversarial examples," in *Association for the Advancement of Artificial Intelligence*, 2020, pp. 3601–3608.
- [34] C. A. Desoer and M. Vidyasagar, *Feedback systems: input-output properties*. SIAM, 1975, vol. 55.
- [35] P. L. Bartlett, D. J. Foster, and M. J. Telgarsky, "Spectrally-normalized margin bounds for neural networks," in *Advances in Neural Information Processing Systems*, 2017, pp. 6240–6249.
- [36] S. Zhou and A. P. Schoellig, "An analysis of the expressiveness of deep neural network architectures based on their Lipschitz constants," *arXiv preprint arXiv:1912.11511*, 2019.
- [37] T. Huster, C.-Y. J. Chiang, and R. Chadha, "Limitations of the Lipschitz constant as a defense against adversarial examples," in *Joint European Conference on Machine Learning and Knowledge Discovery in Databases*. Springer, 2018, pp. 16–29.
- [38] H. Qian and M. N. Wegman, "L₂-nonexpansive neural networks," *International Conference on Learning Representations (ICLR)*, 2019.
- [39] H. Gouk, E. Frank, B. Pfahringer, and M. J. Cree, "Regularisation of neural networks by enforcing Lipschitz continuity," *Machine Learning*, vol. 110, no. 2, pp. 393–416, 2021.
- [40] A. Russo and A. Proutiere, "Optimal attacks on reinforcement learning policies," *arXiv preprint arXiv:1907.13548*, 2019.
- [41] A. Virmaux and K. Scaman, "Lipschitz regularity of deep neural networks: analysis and efficient estimation," in *Advances in Neural Information Processing Systems*, vol. 31, 2018.
- [42] M. Fazlyab, A. Robey, H. Hassani, M. Morari, and G. Pappas, "Efficient and accurate estimation of Lipschitz constants for deep neural networks," in *Advances in Neural Information Processing Systems*, 2019, pp. 11 423–11 434.
- [43] I. R. Manchester, "Contracting nonlinear observers: Convex optimization and learning from data," in *2018 American Control Conference (ACC)*. IEEE, 2018, pp. 1873–1880.
- [44] B. Yi, R. Wang, and I. R. Manchester, "Reduced-order nonlinear observers via contraction analysis and convex optimization," in *2020 American Control Conference (ACC)*. IEEE, 2020.
- [45] J. P. Hespanha, *Linear Systems Theory*. Princeton university press, 2018.
- [46] K. Fujimoto and T. Sugie, "Characterization of all nonlinear stabilizing controllers via observer-based kernel representations," *Automatica*, vol. 36, no. 8, pp. 1123–1135, Aug. 2000.
- [47] A. Alessio and A. Bemporad, "A Survey on Explicit Model Predictive Control," in *Nonlinear Model Predictive Control: Towards New Challenging Applications*, ser. Lecture Notes in Control and Information Sciences, L. Magni, D. M. Raimondo, and F. Allgöwer, Eds. Berlin, Heidelberg: Springer, 2009, pp. 345–369.
- [48] R. S. Sutton and A. G. Barto, *Reinforcement Learning: An Introduction*. MIT press, 2018, vol. 2.
- [49] F. Ferraguti, N. Preda, A. Manurung, M. Bonfè, O. Lambercy, R. Gassert, R. Muradore, P. Fiorini, and C. Secchi, "An Energy Tank-Based Interactive Control Architecture for Autonomous and Teleoperated Robotic Surgery," *IEEE Transactions on Robotics*, vol. 31, no. 5, pp. 1073–1088, Oct. 2015.
- [50] E. Shahriari, A. Kramerberger, A. Gams, A. Ude, and S. Haddadin, "Adapting to contacts: Energy tanks and task energy for passivity-based dynamic movement primitives," in *2017 IEEE-RAS 17th International Conference on Humanoid Robotics (Humanoids)*, Nov. 2017, pp. 136–142.
- [51] Y. Kawano and M. Cao, "Design of Privacy-Preserving Dynamic Controllers," *IEEE Transactions on Automatic Control*, vol. 65, no. 9, pp. 3863–3878, Sep. 2020.
- [52] S. Burer and R. D. Monteiro, "A nonlinear programming algorithm for solving semidefinite programs via low-rank factorization," *Mathematical Programming*, vol. 95, no. 2, pp. 329–357, 2003.
- [53] D. P. Kingma and J. Ba, "Adam: A Method for Stochastic Optimization," *International Conference for Learning Representations (ICLR)*, Jan. 2017.
- [54] G. Calafiore and F. Dabbene, "Control design with hard/soft performance specifications: A Q-parameter randomization approach," *International Journal of Control*, vol. 77, no. 5, pp. 461–471, Mar. 2004.
- [55] M. Buehner and P. Young, "A tighter bound for the echo state property," *IEEE Transactions on Neural Networks*, vol. 17, no. 3, pp. 820–824, May 2006.
- [56] I. B. Yildiz, H. Jaeger, and S. J. Kiebel, "Re-visiting the echo state property," *Neural Networks*, vol. 35, pp. 1–9, Nov. 2012.
- [57] M. Revay, R. Wang, and I. R. Manchester, "Recurrent equilibrium networks: Unconstrained learning of stable and robust dynamical models," *arXiv preprint arXiv:2104.05942v1*, 2021.
- [58] S. Bai, J. Z. Kolter, and V. Koltun, "Deep equilibrium models," in *Advances in Neural Information Processing Systems*, 2019, pp. 690–701.
- [59] E. Winston and J. Z. Kolter, "Monotone operator equilibrium networks," in *Advances in Neural Information Processing Systems*, vol. 33, 2020, pp. 10 718–10 728.
- [60] M. Revay, R. Wang, and I. R. Manchester, "Lipschitz bounded equilibrium networks," *arXiv:2010.01732*, 2020.

- [61] L. El Ghaoui, F. Gu, B. Travacca, A. Askari, and A. Y. Tsai, “Implicit deep learning,” *arXiv:1908.06315*, 2019.
- [62] E. K. Ryu and S. Boyd, “Primer on monotone operator methods,” *Appl. Comput. Math.*, vol. 15, no. 1, pp. 3–43, 2016.
- [63] I. Goodfellow, Y. Bengio, and A. Courville, *Deep learning*. MIT press, 2016.
- [64] A. Megretski and A. Rantzer, “System analysis via integral quadratic constraints,” *IEEE Trans. Autom. Control*, vol. 42, no. 6, pp. 819–830, Jun. 1997.
- [65] Y.-C. Chu and K. Glover, “Bounds of the induced norm and model reduction errors for systems with repeated scalar nonlinearities,” *IEEE Transactions on Automatic Control*, vol. 44, no. 3, pp. 471–483, 1999.
- [66] F. J. D’Amato, M. A. Rotea, A. Megretski, and U. Jönsson, “New results for analysis of systems with repeated nonlinearities,” *Automatica*, vol. 37, no. 5, pp. 739–747, 2001.
- [67] V. V. Kulkarni and M. G. Safonov, “All multipliers for repeated monotone nonlinearities,” *IEEE Transactions on Automatic Control*, vol. 47, no. 7, pp. 1209–1212, 2002.
- [68] B. Wahlberg and P. M. Mäkilä, “On approximation of stable linear dynamical systems using Laguerre and Kautz functions,” *Automatica*, vol. 32, no. 5, pp. 693–708, May 1996.
- [69] M. Schoukens and K. Tiels, “Identification of block-oriented nonlinear systems starting from linear approximations: A survey,” *Automatica*, vol. 85, pp. 272–292, 2017.
- [70] F. Giri and E.-W. Bai, *Block-oriented nonlinear system identification*. Springer, 2010, vol. 1.
- [71] M. Schoukens, A. Marconato, R. Pintelon, G. Vandersteen, and Y. Rolain, “Parametric identification of parallel wiener–hammerstein systems,” *Automatica*, vol. 51, pp. 111–122, 2015.
- [72] J. Noël and M. Schoukens, “F-16 aircraft benchmark based on ground vibration test data,” *Workshop on Nonlinear System Identification Benchmarks*, pp. 15–19, 2017.
- [73] M. Schoukens and J. Noël, “Wiener-hammerstein benchmark with process noise,” *Workshop on Nonlinear System Identification Benchmarks*, pp. 19–23, 2017.
- [74] M. Revay, “Robust RNN,” May 2021. [Online]. Available: <https://github.com/imanchester/RobustRNN.git>
- [75] M. Innes, “Don’t unroll adjoint: Differentiating ssa-form programs,” *arXiv preprint arXiv:1810.07951*, 2018.
- [76] M. Schoukens and J. Noël, “Wiener-hammerstein benchmark with process noise,” in *Workshop on nonlinear system identification benchmarks*, 2016, pp. 15–19.
- [77] A. Astolfi, D. Karagiannis, and R. Ortega, *Nonlinear and Adaptive Control with Applications*. Springer Science & Business Media, 2007.
- [78] H. K. Khalil, *High-Gain Observers in Nonlinear Feedback Control*. SIAM, 2017.
- [79] P. Bernard, *Observer Design for Nonlinear Systems*. Springer, 2019.
- [80] R. Featherstone, *Rigid Body Dynamics Algorithms*. Springer, 2014.
- [81] B. H. Gilding and R. Kersner, *Travelling Waves in Nonlinear Diffusion-Convection Reaction*. Birkhauser, 2012, vol. 60.
- [82] T. Meurer, “On the extended luenberger-type observer for semilinear distributed-parameter systems,” *IEEE Transactions on Automatic Control*, vol. 58, no. 7, pp. 1732–1743, 2013.
- [83] D. Youla, H. Jabr, and J. Bongiorno, “Modern Wiener-Hopf design of optimal controllers—Part II: The multivariable case,” *IEEE Transactions on Automatic Control*, vol. 21, no. 3, pp. 319–338, Jun. 1976.
- [84] N. Agarwal, B. Bullins, E. Hazan, S. Kakade, and K. Singh, “Online Control with Adversarial Disturbances,” in *International Conference on Machine Learning*. PMLR, May 2019, pp. 111–119.
- [85] M. Simchowitz, K. Singh, and E. Hazan, “Improper Learning for Non-Stochastic Control,” in *Conference on Learning Theory*. PMLR, Jul. 2020, pp. 3320–3436.
- [86] X. Glorot and Y. Bengio, “Understanding the difficulty of training deep feedforward neural networks,” in *Proceedings of the thirteenth international conference on artificial intelligence and statistics*. JMLR Workshop and Conference Proceedings, 2010, pp. 249–256.
- [87] M. M. Tobenkin, I. R. Manchester, and A. Megretski, “Convex parameterizations and fidelity bounds for nonlinear identification and reduced-order modelling,” *IEEE Transactions on Automatic Control*, vol. 62, no. 7, pp. 3679–3686, 2017.